A head-to-head comparison of conjugation methods for VHHs: Random maleimide-thiol coupling versus controlled click chemistry

Marc V.A. van Moorsel[a], Rolf T. Urbanus[a,b,c], S. Verhoef[a], C.A. Koekman[a], Maurice Vink[a], T. Vermonden[d], Coen Maas[a], Gerard Pasterkamp[a], Raymond M. Schiffelers[a,*]

[a] Department of Clinical Chemistry and Hematology, University Medical Center Utrecht, Utrecht University, Utrecht, The Netherlands
[b] Van Creveldkliniek, University Medical Center Utrecht, Utrecht University, Utrecht, The Netherlands
[c] Van Creveld Laboratory for Thrombosis and Haemostasis, University Medical Center Utrecht, Utrecht University, Utrecht, The Netherlands
[d] Department of Pharmaceutical Sciences, Utrecht Institute for Pharmaceutical Sciences (UIPS), Utrecht University, Utrecht, The Netherlands

ABSTRACT

Targeted delivery of therapeutics is an attractive strategy for vascular diseases. Recently, variable domains of heavy-chain-only antibodies (VHHs) have gained momentum as targeting ligands to achieve this. Targeting ligands need adequate conjugation to the preferred delivery platform. When choosing a conjugation method, two features are critical: a fixed and specified stoichiometry and an orientation of the conjugated targeting ligand that preserves its functional binding capacity. We here describe a comparison of popular maleimide-thiol conjugation with state-of-the-art "click chemistry" for conjugating VHHs. First, we demonstrate the modification of VHHs with azide via Sortase A mediated transpeptidation. Subsequently, optimal clicking conditions were found at a temperature of 50 °C, using a 3:1 M ratio of DBCO-PEG:VHH-azide and an incubation time of 18 h. Second, we show that stoichiometry was controllable with click chemistry and produced defined conjugates, whereas maleimide-thiol conjugation resulted in diverse reaction products. In addition, we show that all VHHs – independent of the conjugation method or conjugated residue – still specifically bind their cognate antigen. Yet, VHH's functional binding capacities after click chemistry were at least equal or better than maleimide thiol conjugates. Together these data underline that click chemistry is superior to maleimide-thiol conjugation for conjugating targeting ligands.

1. Introduction

For therapeutics with a small therapeutic window, targeted delivery can minimize adverse effects on healthy tissue and can maximize accumulation of therapeutic effects at the site of disease (Rosenblum et al., 2018; Strobel et al., 2018). While targeted delivery is commonly investigated in cancer treatment, it can also be an attractive strategy in vascular diseases such as atherosclerosis, restenosis, and aneurysm formation. Intraluminal antigens are well accessible for intravenously administered targeting ligands and, as only small regions of the blood vessels are affected, targeted delivery is expected to have substantial impact on the target/non-target tissue ratio (Molloy et al., 2017; Ridker et al., 2011; Strobel et al., 2018). Next to targeted delivery of therapeutics, disease-related biomarkers can be targeted with imaging enhancers to diagnose specific cardiovascular diseases. Previous efforts included targeting of vascular cell adhesion molecule-1 (VCAM-1) to diagnose inflamed atherosclerotic plaques (Bala et al., 2016; Broisat et al., 2012), intercellular adhesion molecule-1 (ICAM-1) to diagnose acute cardiac transplant rejection (Weller et al., 2003) and activated integrin glycoprotein IIb/IIIa (αIIbβ3) on platelets to diagnose (athero) thrombosis (Meier et al., 2015; von zur Muhlen et al., 2008), pulmonary embolism (Heidt et al., 2016) or cardiac ischemia (Ziegler et al., 2016). The targeted delivery of imaging enhancers for diagnostic purposes is especially interesting for asymptomatic cardiovascular patients, as it enables (pharmaceutical) actions to prevent acute events.

Targeted delivery can be accomplished with ligands that specifically interact with the compartment, organ, tissue or cell of interest (Atukorale et al., 2017). Antibodies are highly suitable for this purpose due to the high affinity and specificity of their target recognition motifs (Hudson and Souriau, 2003). Recently, variable domains of heavy chain only antibodies (VHHs) have gained momentum as targeting ligands in cardiovascular diseases (Bala et al., 2016; Broisat et al., 2012). VHHs

are theoretically superior to antibodies for multiple reasons. First, VHHs have smaller molecular size (~15kDa) than antibodies (~150kDa), which facilitates the target penetration of conjugated therapeutics. Second, VHHs have higher specificity for conformational epitopes of antigens than antibodies (Hagemeyer et al., 2009). Third, VHHs lack the Fc-domain, so the activation of Fc receptor–expressing cells is prevented. This activation can result in undesirable cytokine release and consequent adverse effects. Finally, VHHs are less immunogenic than antibodies (Pansieri et al., 2018).

To use VHHs as targeting ligands, they need – similarly as any other ligand – adequate conjugation to the preferred delivery platform, for example a nanoparticle delivery system or polymer. When choosing a conjugation method, two features are critical: a fixed and specified stoichiometry (i.e. the number of defined products formed with a fixed number of reactants) and an orientation of the conjugated targeting ligand that preserves its functional binding capacity.

The most popular approach for the conjugation of proteins as targeting ligands is based on a maleimide-thiol reaction. For this reaction to occur, targeting ligands need to contain a reactive thiol residue. Thiols can be introduced by modifying ligands with N-succinimidyl-S-acetyl-thioacetate (SATA). SATA molecules bind to primary amines on the targeting ligand, usually lysine residues. The introduced thiol residue is then activated via deacetylation with hydroxylamine, allowing the formation of a covalent bond with maleimide conjugated acceptor molecules. Theoretically, maleimide-thiol conjugation has two major shortcomings. First, there is limited control over the stoichiometry, as multiple maleimide molecules can be conjugated when targeting ligands contain multiple primary amines. Second, the orientation of the conjugated acceptor molecules is not controlled, as primary amines are generally randomly positioned within the targeting ligand (Oude Blenke et al., 2015). This could result in steric hindrance and thus a reduced binding capacity of the targeting ligand. Due to the random distribution of the primary amines, maleimide-thiol conjugation also necessitates a re-optimization for every new protein that is to be conjugated. Engineering targeting ligands with an additional (c-terminal) cysteine residue is repeatedly described as a solution. However, introducing cysteine residues can interfere with native disulfides (intramolecular) or result in polymerization (intermolecular). In addition, the engineered cysteines are prone to cysteinylation and glutathionylation. When reducing these oxidized forms for conjugation, it is often difficult not to reduce native disulfides as well (Peciak et al., 2019).

Copper free strain-promoted azide alkyne cycloaddition (SPAAC) – generally referred to as "click chemistry" – is a state-of-the-art conjugation method and is associated with a defined one-on-one stoichiometry and a site-directed orientation of the conjugated targeting ligand (A little less conjugation, a little more accuracy, 2016). Similar as for the maleimide-thiol method, this method also requires the modification of targeting ligands, in this case with either a cycloalkyne or an azide residue. Azide residues can be introduced at the C- or N-terminus of any targeting ligand via Sortase A mediated transpeptidation as described previously (Witte et al., 2013). To introduce azide to VHHs, VHHs need to contain a LPXTG sequence. Sortase A recognizes this sequence and replaces the glycine amino acid with Gly_3-azide, forming VHH-azide. Subsequently, the azide residue "clicks" to dibenzocyclooctyne (DBCO) conjugated acceptor molecules.

We here describe a comparison of maleimide-thiol conjugation with optimized click chemistry for conjugating VHHs directed to intraluminal proteins to various delivery platforms. We compared the conjugates with respect to coupling stoichiometry and antigen binding capacity.

2. Materials and methods

2.1. Materials

Biotin-maleimide, DBCO-PEG4-biotin and N-succinimidyl-S-acetyl-

thioacetate (SATA) were from Sigma-Aldrich (Saint Louis, Missouri, USA). Luminol, Nunc 96-well maxisorp microtiter plates and Zeba Spin 7 kDa desalting columns were from Thermo Scientific (Waltham, Massachusetts, USA). Spectramax L and Spectramax M2 were from Molecular Devices (San Jose, California, USA). Streptavidin-polyHRP and secondary rabbit anti-mouse HRP antibody were from Agilent Technologies (Santa Clara, California, USA). BL21 pLyss *E. Coli* was obtained from Invitrogen (Carlsbad, California, USA) and vector pet30b-7M SrtA (plasmid # 51141), encoding a modified, calcium-independent Sortase A from *S. aureus* was a gift from Hidde Ploegh and ordered from Addgene (Watertown, Massachusetts, USA). DBCO-PEG (20 kDa) was from Jena Bioscience (Jena, Germany) and mPEG-maleimide (20 kDa) was from Broadpharm (Waples, San Diego, USA). DABCYL-LPETG-EDANS was from AnaSpec (Waddinxveen, the Netherlands). Gly_3-azide was from IRIS Biotech GmbH (Marktredwitz, Germany). Imidazole was from Merck Millipore (Burlington, Massachusetts, USA). Phe-Pro-Arg-chloromethylketone (PPACK) was from Haematologic Technologies (Essex Junction, Vermont, USA). Talon Superflow was from GE Healthcare (Hoevelaken, The Netherlands).

2.2. Synthesis of cloning vectors

Two Llamas (*Llama glama*) were immunized with purified human VWF and fibrin degradation products for four times with weekly intervals. A B-cell bacteriophage library containing the heavy chain-only antibody repertoire of the immunized llamas was prepared, and VHHs were obtained via phage-display as described previously (de Maat et al., 2013). For modification with SATA, VHHs were cloned into an engineered pet32a(+)-based prokaryotic expression vector containing an N-terminal Shine-Dalgarno sequence, a PelB leader peptide, a $(His)_8$ purification tag and a tobacco etch virus (TEV) cleavage site to remove the his-tag after purification. A c-myc-tag was cloned at the C-terminus of the VHH for detection purposes. For Sortase-based modification, VHHs were cloned in an alternative vector (own production), which contained an N-terminal Shine Dalgarno sequence, a PelB leader peptide and a C-terminal c-myc-tag followed by a $(Gly_4$-Ser$)_2$ linker, a Leu-Pro-Glu-Thr-Gly (LPETG) sortase tag and a $(His)_8$-purification tag.

2.3. Purification of VHHs

VHHs were produced in *E. coli* strain BL21 pLyss with autoinduction as described by Studier (2005) in a bioreactor. VHHs were purified with immobilized metal affinity chromatography (IMAC) on Talon Superflow. VHHs produced for SATA modification were incubated with TEV protease (own production) to remove the his-tag. Excess TEV protease and uncleaved VHHs were removed with IMAC. All VHHs were subjected to size exclusion chromatography. Resulting VHH preparations were > 95% pure, as estimated with SDS-PAGE and Coomassie Brilliant Blue protein staining.

2.4. Synthesis, purification and functionality of Sortase a (SrtA)

Sortase A was expressed in *E. coli* strain BL21 pLyss with an autoinduction protocol and was purified as described (Antos et al., 2017). Enzymatic activity of Sortase A was confirmed with fluorescent substrate DABCYL-LPETG-EDANS as described (Mazmanian et al., 2002).

2.5. Maleimide-thiol conjugation

N-succinimidyl-S-acetyl-thioacetate (SATA) was dissolved in DMSO and incubated in a 6:1 SATA:VHH molar ratio overnight at room temperature (RT). Unbound SATA was then removed with size exclusion chromatography on Zeba spin 7 kDa desalting columns. Thiol groups were deacetylated with 0.5 M hydroxylamine-HCL, 0.5 M HEPES-buffered saline (HBS; 10 mM HEPES, 150 mM NaCl, pH 7.4), 25 mM EDTA

for 90 min at RT. Deacetylated VHHs were immediately incubated with maleimide conjugated acceptor molecules, including mPEG-maleimide (20 kDa) and biotin-maleimide. Conjugation was performed in a 10:1 maleimide:VHH molar ratio for 90 min at RT. Excess acceptor molecules were removed with Zeba spin 7 kDa desalting columns.

2.6. Click chemistry conjugation

Gly$_3$-Lys-azide was enzymatically added to the C-terminus of the VHHs as described (Antos et al., 2017). In short, 50 µM VHH containing a LPETG tag, 250 µM Gly$_3$-Lys-azide and 2,5 µM SrtA were incubated in tris-buffered saline (TBS; 50 mM Tris, 150 mM NaCl, pH7.4) for 30 min at RT. The resulting VHH-azide intermediates were subjected to IMAC on Talon Superflow to remove SrtA and unmodified VHHs, followed by size exclusion chromatography on Zeba spin 7 kDa desalting columns to remove excess Gly$_3$-Lys-azide. Subsequently, VHH-azide intermediates were allowed to react with DBCO conjugated acceptor molecules, including DBCO-PEG (20 kDa) or DBCO-PEG4-biotin (4 kDa). Reactions were performed at a VHH concentration of 80 µM as described (Witte et al., 2013). We varied clicking conditions for temperature, DBCO:azide molar ratio and incubation times as indicated. Excess DBCO-containing biotin molecules were removed with Zeba spin 7 kDa desalting columns.

For both conjugation methods, the resulting conjugation products were directly used for experiments. Conjugation efficiency was monitored with SDS-PAGE and Coomassie Brilliant Blue protein staining. Reaction efficiency was estimated with densitometry, measured via ImageJ Software V1.0. Here, the amount of conjugates as a fraction of the total protein was calculated for each lane. Degrees of biotin conjugation were quantified via Pierce Biotin Quantitation kit.

2.7. Solid phase binding studies

Nunc 96-well maxisorp microtiter plates were either coated with human VWF (5 µg/mL) in phosphate-buffered saline (PBS; 137 mM NaCl, 2.7 mM KCl, 9.2 mM Na2HPO4, 1.76 mM KH2PO4, pH7.4) or with fibrin in HEPES-buffered saline (HBS; 10 mM HEPES, 150 mM NaCl, pH 7.4), by incubating with human fibrinogen (500 µg/mL) and human α-thrombin (40 U/mL). Plates were incubated overnight at 4 °C and blocked with 2% BSA in PBS for VWF binding assays or HBS for fibrin binding assays for 1 h at RT. Blocking buffers for fibrin binding assays additionally contained 100 µM Phe-Pro-Arg-chloromethylketone (PPACK) to inhibit residual thrombin activity.

Plates were washed thoroughly with either PBS with 0.1% tween-20 (VWF coat), or HBS with 0.1% tween-20 (fibrin coat). Conjugated VHH samples were subsequently diluted in blocking buffer to the indicated concentrations and incubated for 2 h at RT. Plates were washed thoroughly, and incubated with either streptavidin-polyHRP for 1 h at RT to detect biotin, or mouse anti-c-myc (clone 9E10; 1 µg/mL), followed by rabbit anti-mouse HRP, both for 1 h at RT. Biotin was detected with luminol on a Spectramax L. Anti-c-myc was detected with TMB. Colorimetric reactions were stopped with 0.1 M H$_2$SO$_4$. Absorbance was measured on a Spectramax M2 at 450 nm. Binding data were fitted with non-linear regression with Graphpad Prism software (v7.04). Langmuir 1:1 binding was assumed for all VHH-antigen interactions. Data are expressed as dissociation constants (K$_D$).

2.8. Statistical analysis

PEG conjugated VHHs included three samples (unmodified VHHs, VHHs conjugated via maleimide-thiol and VHHs conjugated via click chemistry) and mean values were analyzed by one-way ANOVA. Biotin conjugated VHHs included two samples (VHHs conjugated via maleimide-thiol and VHHs conjugated via click chemistry) and mean values were analyzed by Welch's T-Test. Results were considered statistically significant at p ≤ 0.05.

3. Results and discussion

3.1. VHHs were successfully modified with azide and "clicked" under optimized conditions

Click chemistry requires the modification of targeting ligands with azide, which was achieved via Sortase A mediated transpeptidation of glycine amino acids from VHH-LPETG with Gly$_3$-azide, forming VHH-azide. In front of the LPETG sequence, a glycine linker (GGGGS)$_2$ was constructed to prevent steric hindrance for SrtA (Antos et al., 2017). The resulting reaction efficiency was 83.6% calculated by reaction products found in flow through (Fig. 1A). As expected, the reaction did not progress when Sortase A was absent.

Next, we determined the optimal "click" conditions to conjugate residues to VHH-azide, in this case DBCO-Polyethylene Glycol (PEG) (20 kDa). PEG is an often used polymer to increase therapeutic half-life for peptides or proteins that are below the renal clearance cut-off. We clicked DBCO-PEG to three different VHHs and analyzed the effects of temperature, the molar ratio of DBCO-PEG:VHH-azide and incubation time (Fig. 1B–D). When investigating one variable, other variables were kept constant (room temperature; 3:1 M ratio; 18 h). Click reactions readily occurred at 4 °C, but yields increased at higher temperatures. In addition, increasing the molar ratio DBCO-PEG:VHH-azide increased the reaction efficiency up to a 3:1 ratio. At higher ratios, the reaction efficiency decreased. Lastly, click reactions started directly after incubation and highest yields were obtained with increasing incubation times.

Conclusively, Sortase A mediated transpeptidation was highly efficient for modifying VHHs with azide and optimal clicking conditions were found at a temperature of 50 °C, using a 3:1 M ratio DBCO-PEG:VHH-azide and incubation for 18 h.

3.2. Stoichiometry is controllable with click chemistry, but not with thiol-based conjugation

Next, we compared the conjugate-to-VHH ratio obtained after maleimide-thiol conjugation with that obtained after click chemistry. First, three different VHHs were biotinylated and the mean number of biotin conjugates per VHH was determined (Table 1). Each VHH contained more than one lysine residue, which could theoretically result in more than one conjugate per VHH when maleimide-thiol conjugation was applied. Indeed, maleimide-thiol conjugation resulted in > 1 biotin conjugates per VHH, indicating a multiple-to-one stoichiometry with diverse reaction products. In contrast, click chemistry resulted in < 1 biotin conjugate per VHH, indicating that the majority of VHHs either bound zero or one biotin residue. The protein staining shown in Fig. 1 – where one reaction product is formed – supports this notion.

To investigate stoichiometry in greater detail, VHHs were PEGylated via both methods, resulting in large molecular weight shifts upon successful conjugation. Indeed, SDS-PAGE showed 1–4 PEG moieties conjugated to VHH with maleimide-thiol conjugation (Fig. 2A), but a one-to-one stoichiometry with click chemistry (Fig. 2B). Both methods showed a small percentage of unconjugated VHH. Conclusively, stoichiometry was controllable with click chemistry and produced a defined conjugate, but maleimide-thiol conjugation resulted in diverse reaction products.
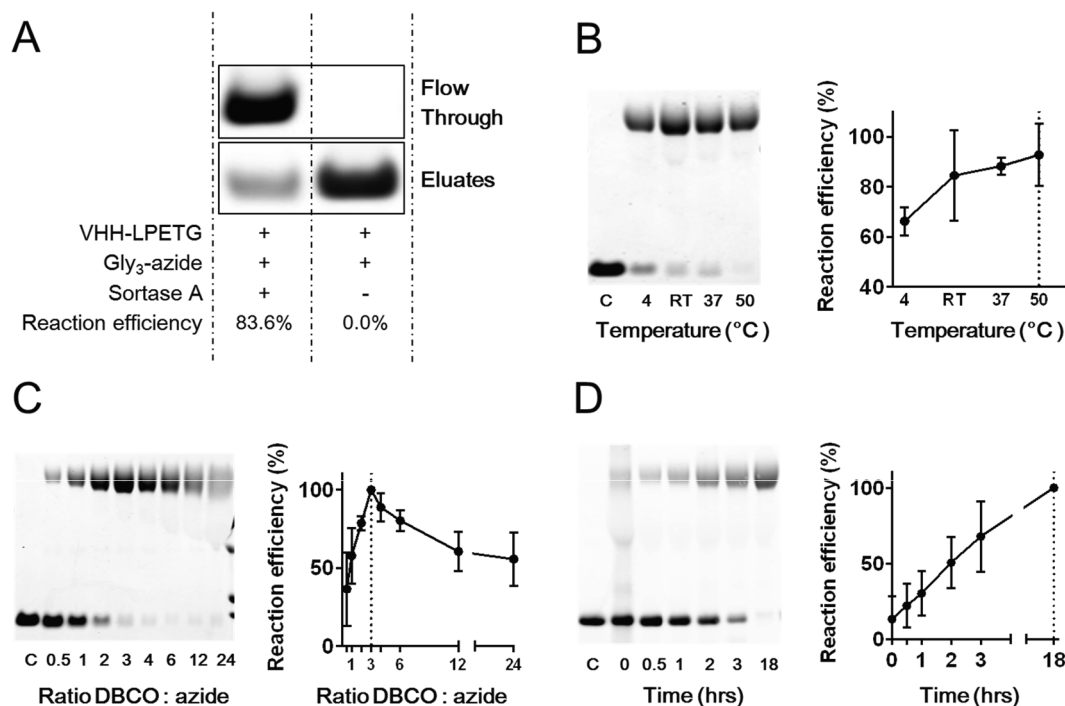
Fig. 1. VHHs were successfully modified with azide and "clicked" under optimized conditions. Samples were subjected to IMAC on Talon Superflow and flow through was collected. Subsequently, talon was eluted with 500 mM imidazole and eluates were collected. (A) Sortase A mediated transpeptidation showed a reaction efficiency of 83.6%. Next, we clicked VHH-azide to DBCO-PEG (20 kDa) under various conditions, including (B) temperature, (C) molar ratio DBCO-PEG:VHH-azide and (D) incubation time. When investigating one variable, other variables were kept constant. Graphs represent a total of n = 3 experiments with VHH NT (non-targeting), VHH a-sVWF or VHH a-FIBR and were expressed as percentage ± SD of the maximal efficient condition (set at 100%). Concomitant protein gels represent a single VHH reaction. For all situations, reaction efficiency was determined by intensity, measured via ImageJ Software V1.0.

Table 1

Quantification analysis supports that click chemistry, and not maleimide-thiol conjugation, results in one-to-one stoichiometry. Data represents the average of biotin molecules per VHH from n = 3 experiments and is expressed as average ± SD.

		Conjugate: VHH ratio	
	No. of available lysine residues	Maleimide thiol conjugation	Click chemistry
VHH NT (non-targeting)	6	1.33 ± 0.10	0.64 ± 0.22
VHH a-sVWF	6	1.80 ± 0.36	0.83 ± 0.31
VHH a-FIBR	4	1.36 ± 0.21	0.69 ± 0.22

3.3. Functional binding capacities are preserved for both conjugation methods

Lastly, we performed solid phase binding assays in order to investigate how conjugation with both methods influenced the apparent antigen binding affinity of VHHs (K_D). Theoretically, the binding affinity can be impaired by steric hindrance. We selected VHHs that lacked lysine-residues within the antigen binding region because their binding affinity would certainly be affected when maleimide-thiol conjugation was applied. This would provide an advantage to the click chemistry approach that is not entirely reflecting the true improvement as lysine residues in the binding pocket are usually replaced to prevent this from happening. The performed binding assays included VWF and fibrin coats and VHHs were conjugated to PEG (20 kDa) and biotin via both conjugation methods. All VHHs – independent of whether they were conjugated to PEG (20 kDa) or biotin – bound their cognate antigen in a

sigmoidal dose-dependent manner, which underlines specific binding (Fig. 3A–D).

The apparent binding affinity of VHH a-sVWF-PEG (20 kDa) conjugates to coated VWF was impaired by maleimide-thiol conjugation, but not after click chemistry (Fig. 3A). Clicked conjugates demonstrated a > 10-fold lower K_D to VWF than maleimide-thiol conjugates. For the much smaller biotin conjugates the difference was not significant (Fig. 3B). The apparent binding affinity of VHH a-FIBR-PEG (20 kDa) conjugates was substantially impaired (> 10-fold) for both conjugation methods (Fig. 3C). Also for biotin conjugated VHHs, both conjugation methods resulted in similar binding profiles (Fig. 3D). Non-targeting VHH NT showed indeed no binding for both coatings and none of the VHHs showed a-specific binding on non-coated plates (Fig. 3A & C). Conclusively, after click chemistry VHHs' functional binding capacities were equal or better than maleimide thiol conjugates.

4. Conclusion

We applied Sortase A mediated transpeptidation to introduce an azide functional group to VHHs with high efficiency. We showed that optimal conditions for the subsequent click reaction include a temperature of 50 °C, a 3:1 M ratio DBCO:azide and incubation for 18 h. Subsequently, we compared click chemistry with maleimide-thiol conjugation as methods to conjugate VHHs. We showed a preferred one-to-one defined stoichiometry for click chemistry and a multiple-to-one stoichiometry for maleimide-thiol conjugation with multiple reaction products. Additionally, we showed that conjugation via both methods decreased VHHs' binding capacity, but that a dose-dependent and functional capacity to their cognate antigen is preserved. Remaining binding capacities after click chemistry were, however, equal or better
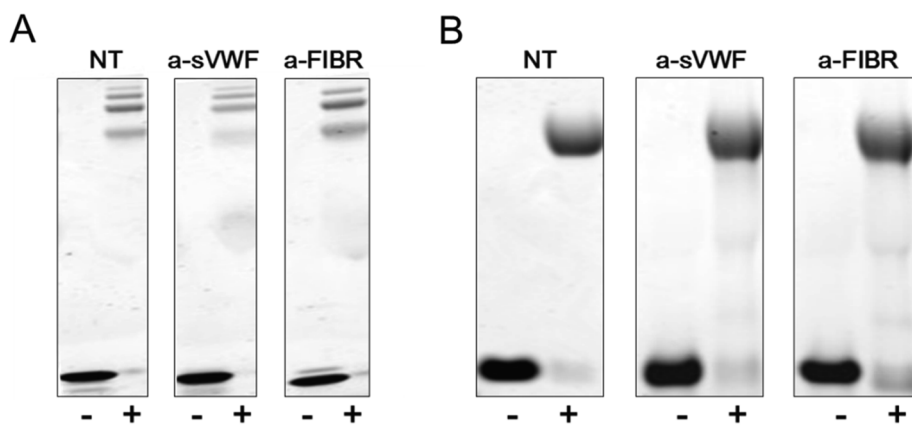
Fig. 2. Protein gels confirm that click chemistry, and not maleimide-thiol conjugation, resulted in one-to-one stoichiometry. SDS-page of VHH-PEG (20 kDa) conjugates (+) via (A) maleimide-thiol conjugation or (B) click chemistry. Negative controls (−) included unmodified VHHs.
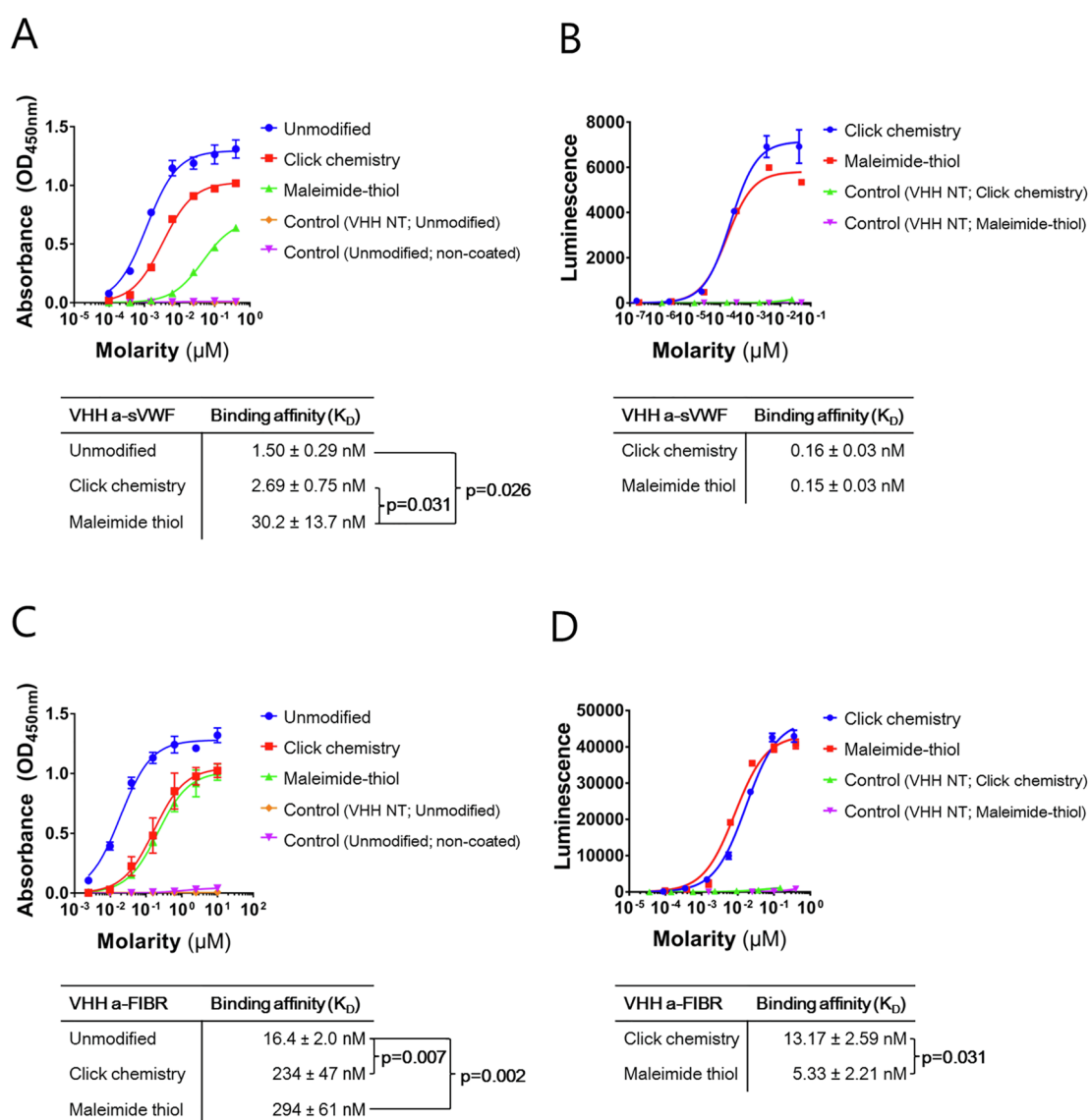

Fig. 3. VHHs' functional binding capacities after click chemistry were equal or better than maleimide thiol conjugates. Four solid phase binding assays were performed, including the following conjugate combinations (A) VHH a-sVWF conjugated to PEG (20 kDa); (B) VHH a-sVWF conjugated to biotin; (C) VHH a-FIBR conjugated to PEG (20 kDa); and (D) VHH a-FIBR conjugated to biotin. Biotin conjugates were measured via the biotin residue and PEG (20 kDa) conjugates were measured via their c-myc-tag. For PEG (20 kDa) conjugates we also included unmodified VHH. Graphs represent single *in triplo* experiments per conjugate combination. Concomitant K_D values represent n = 3 experiments per conjugate combination and were expressed as average ± SD. (COLOR FIGURE).

than maleimide thiol conjugates.

In summary, when targeting ligands contain at least one primary amine residue, maleimide-thiol conjugation can be accomplished without any genetic modification of the targeting ligand. Contrarily, click chemistry requires targeting ligands to be genetically modified with a LPXTG sequence, but result in a predefined stoichiometry and a site-directed orientation of the conjugated targeting ligand. Consequently, click chemistry is considered favorable to produce uniform VHH conjugates with preserved functional antigen binding capacity.

Acknowledgments

Declaration of Competing Interest

None.

References

A little less conjugation, a little more accuracy, 2016. A little less conjugation, a little more accuracy. Nat. Chem. 8 (2), 91–92. https://doi.org/10.1038/nchem.2448.

Antos, J.M., Ingram, J., Fang, T., Pishesha, N., Truttmann, M.C., Ploegh, H.L., 2017. Site-specific protein labeling via sortase-mediated transpeptidation. Curr. Protoc. Protein Sci. 89, 15.3.1–15.3.19. https://doi.org/10.1002/cpps.38.

Atukorale, Prabhani U., Covarrubias, Gil, Bauer, Lisa, Karathanasis, Efstathios, 2017. Vascular targeting of nanoparticles for molecular imaging of diseased endothelium. Adv. Drug Deliver. Rev. 113, 141–156. https://doi.org/10.1016/j.addr.2016.09.006.

Bala, Gezim, Blykers, Anneleen, Xavier, Catarina, Descamps, Benedicte, Broisat, Alexis, Ghezzi, Catherine, Fagret, Daniel, Van Camp, Guy, Caveliers, Vicky, Lahoutte, Christian Vanhove Tony, Droogmans, Steven, Cosyns, Bernard, Devoogdt, Nick, Hernot, Sophie, 2016. Targeting of vascular cell adhesion molecule-1 by ^{18}F-labelled nanobodies for PET/CT imaging of inflamed atherosclerotic plaques. Eur. Heart J. - Cardiovasc. Imaging 17 (9), 1001–1008. https://doi.org/10.1093/ehjci/jev346.

Broisat, Alexis, Hernot, Sophie, Toczek, Jakub, De Vos, Jens, Riou, Laurent M., Martin, Sandrine, Ahmadi, Mitra, Thielens, Nicole, Wernery, Ulrich, Caveliers, Vicky, Muyldermans, Serge, Lahoutte, Tony, Fagret, Daniel, Ghezzi, Catherine, Devoogdt, Nick, 2012. Nanobodies Targeting Mouse/Human VCAM1 for the Nuclear Imaging of Atherosclerotic Lesions. Circ. Res. 110 (7), 927–937. https://doi.org/10.1161/CIRCRESAHA.112.265140.

de Maat, S., van Dooremalen, S., de Groot, P.G., Maas, C., 2013. A nanobody-based method for tracking factor XII activation in plasma. Thromb. Haemost. 110 (3), 458–468. https://doi.org/10.1160/TH12-11-0792.

Hagemeyer, C. E., Von Zur Muhlen, C., Von Elverfeldt, D., and Peter, K., 2009. Single-chain antibodies as diagnostic tools and therapeutic agents. In Thrombosis and Haemostasis (Vol. 101, pp. 1012–1019). doi: 10.1160/TH08-12-0816.

Heidt, Timo, Ehrismann, Simon, Hövene, Jan-Bernd, Neudorfer, Irene, Hilgendorf, Ingo, Reisert, Marco, Hagemeyer, Christoph E., Zirlik, Andreas, Reinöhl, Jochen, Bode, Christoph, Peter, Karlheinz, von Elverfeldt, Dominik, von zur Muhlen, Constantin, 2016. Molecular imaging of activated platelets allows the detection of pulmonary embolism with magnetic resonance imaging. Sci. Rep. 6, 25044. https://doi.org/10.1038/srep25044.

Hudson, P.J., Souriau, C., 2003. Engineered antibodies. Nat. Med. https://doi.org/10.1038/nm0103-129.

Mazmanian, S.K., Ton-That, H., Su, K., Schneewind, O., 2002. An iron-regulated sortase anchors a class of surface protein during Staphylococcus aureus pathogenesis. Proc. Natl. Acad. Sci. U.S.A. 99 (4), 2293–2298. https://doi.org/10.1073/pnas.032523999.

Meier, S., Pütz, G., Massing, U., Hagemeyer, C.E., von Elverfeldt, D., Meißner, M., Ardipradja, K., Barnert, S., Peter, K., Bode, C., Schubert, R., von zur Muhlen, C., 2015. Immuno-magnetoliposomes targeting activated platelets as a potentially human-compatible MRI contrast agent for targeting atherothrombosis. Biomaterials 53, 137–148. https://doi.org/10.1016/j.biomaterials.2015.02.088.

Molloy, C.P., Yao, Y., Kammoun, H., Bonnard, T., Hoefer, T., Alt, K., Westein, E., 2017. Shear-sensitive nanocapsule drug release for site-specific inhibition of occlusive thrombus formation. J. Thromb. Haemost. 15 (5), 972–982. https://doi.org/10.1111/jth.13666.

Oude Blenke, E., Klaasse, G., Merten, H., Plückthun, A., Mastrobattista, E., Martin, N.I., 2015. Liposome functionalization with copper-free "click chemistry". J. Control. Release 202, 14–20. https://doi.org/10.1016/j.jconrel.2015.01.027.

Pansieri, J., Gerstenmayer, M., Lux, F., Mériaux, S., Tillement, O., Forge, V., Marquette, C., 2018. Magnetic nanoparticles applications for amyloidosis study and detection: a review. Nanomaterials 8 (9), 740. https://doi.org/10.3390/nano8090740.

Peciak, K., Laurine, E., Tommasi, R., Choi, J.W., Brocchini, S., 2019. Site-selective protein conjugation at histidine. Chem. Sci. 10 (2), 427–439. https://doi.org/10.1039/c8sc03355b.

Ridker, P.M., Thuren, T., Zalewski, A., Libby, P., 2011. Interleukin-1β inhibition and the prevention of recurrent cardiovascular events: rationale and design of the canakinumab anti-inflammatory thrombosis outcomes study (CANTOS). Am. Heart J. 162 (4), 597–605. https://doi.org/10.1016/j.ahj.2011.06.012.

Rosenblum, D., Joshi, N., Tao, W., Karp, J.M., Peer, D., 2018. Progress and challenges towards targeted delivery of cancer therapeutics. Nat. Commun. 9 (1), 1410. https://doi.org/10.1038/s41467-018-03705-y.

Strobel, H.A., Qendro, E.I., Alsberg, E., Rolle, M.W., 2018. Targeted delivery of bioactive molecules for vascular intervention and tissue engineering. Front. Pharmacol. 9, 1329. https://doi.org/10.3389/fphar.2018.01329.

Studier, F.W., 2005. Protein production by auto-induction in high density shaking cultures. Protein Expr. Purif. 41 (1), 207–234. https://doi.org/10.1016/j.pep.2005.01.016.

von zur Muhlen, C., von Elverfeldt, D., Moeller, J.A., Choudhury, R.P., Paul, D., Hagemeyer, C.E., Olschewski, M., Becker, A., Neudorfer, I., Bassler, N., Schwarz, M., Bode, C., Peter, K., 2008. Magnetic resonance imaging contrast agent targeted toward activated platelets allows in vivo detection of thrombosis and monitoring of thrombolysis. Circulation 118 (3), 258–267. https://doi.org/10.1161/CIRCULATIONAHA.107.753657.

Weller, Gregory E.R., Lu, Erxiong, Csikari, Melissa M., Klibanov, Alexander L., Fischer, David, Weller, William R., Villanueva, Flordeliza S., 2003. Ultrasound imaging of acute cardiac transplant rejection with microbubbles targeted to intercellular adhesion molecule-1. Circulation 108 (2), 218–224. https://doi.org/10.1161/01.CIR.0000080287.74762.60.

Witte, M.D., Theile, C.S., Wu, T., Guimaraes, C.P., Blom, A.E.M., Ploegh, H.L., 2013. Production of unnaturally linked chimeric proteins using a combination of sortase-catalyzed transpeptidation and click chemistry. Nat. Protoc. 8 (9), 1808–1819. https://doi.org/10.1038/nprot.2013.103.

Ziegler, Melanie, Alt, Karen, Paterson, Brett M., Kanellakis, Peter, Bobik, Alex, Donnelly, Paul S., Hagemeyer, Christoph E., Peter, Karlheinz, 2016. Highly sensitive detection of minimal cardiac ischemia using positron emission tomography imaging of activated platelets. Sci. Rep. 6, 38161. https://doi.org/10.1038/srep38161.